

## One-Step Production of Bioactive Proteins through Simultaneous PEGylation and Refolding

Jianlou Niu,<sup>†,‡</sup> Yanlin Zhu,<sup>‡</sup> Lintao Song,<sup>‡</sup> Yaoyao Xie,<sup>‡</sup> Yi Zhang,<sup>‡</sup> Huiyan Wang,<sup>§</sup> Xiaokun Li,<sup>‡</sup> Bailing Liu,<sup>\*,†</sup> Lu Cai,<sup>‡,||</sup> and Zhifeng Huang<sup>\*,‡</sup>

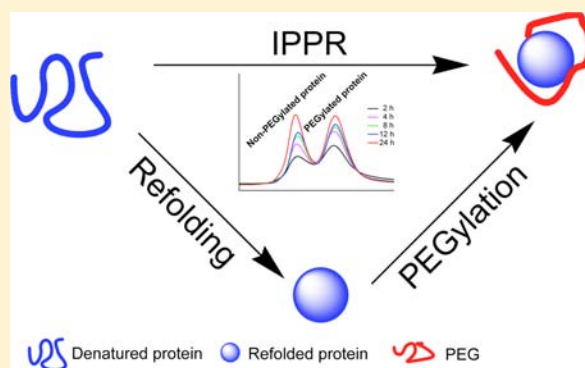
<sup>†</sup>Chengdu Institute of Organic Chemistry, Chinese Academy of Sciences, Chengdu 610041, Sichuan, China

<sup>‡</sup>School of Pharmacy, Wenzhou Medical University, Wenzhou 325035, Zhejiang, China

<sup>§</sup>School of Laboratory Medicine, Jilin Medical College, Jilin 132013, Jilin, China

<sup>||</sup>KCHRI at the Department of Pediatrics, The University of Louisville, Louisville, Kentucky 40202, United States

**ABSTRACT:** Production of protein therapeutics often involves *in vitro* refolding from bacterial inclusion bodies and subsequent PEGylation to improve protein stability and plasma half-life. Here, we devised a novel strategy for one-step production of site-specific mono-PEGylated proteins with good bioactivity and improved biostability by integrating PEGylation and protein refolding (IPPR). Using lysozyme and recombinant human fibroblast growth factor 21 (rhFGF21) as model proteins, we showed that both PEGylation and refolding of denatured proteins have been simultaneously accomplished by IPPR with high efficiency of refolding yield and bioconjugation. PEGylated rhFGF21 by IPPR has a similar capacity as the native rhFGF21 to stimulate glucose uptake in 3T3-L1 cells, but exhibits prolonged blood glucose and triglyceride lowering activity levels in the ob/ob diabetic mouse model. Hence, IPPR will significantly facilitate the generation of protein therapeutics.



### INTRODUCTION

Overexpression of recombinant proteins in different host cells, particularly *Escherichia coli* (*E. coli*), often results in protein product accumulation in inactive and insoluble deposits inside host cells, termed inclusion bodies.<sup>1</sup> Inclusion body proteins must be refolded *in vitro* to gain solubility and bioactivity,<sup>2</sup> although theoretically, an unfolded protein can spontaneously recover its native structure following denaturant dilution. Intermolecular aggregates, as well as partially oxidized or misfolded species, compete against productive refolding, especially in cases of high protein concentration, resulting in low activity yields.<sup>3</sup> To improve *in vitro* protein refolding yield, a number of additives and compounds have been tested, and the molecular mechanisms by which they assist protein refolding have been reported.<sup>4</sup> Among these chemical additives, polyethylene glycol (PEG) has been reported to suppress aggregation by preventing the association of refolding intermediates or unfolded species through hydrophobic interaction.<sup>5</sup>

PEG can also be covalently conjugated to recombinant proteins, a process termed PEGylation,<sup>6</sup> which has been proposed as an effective approach to improve the stability and pharmacokinetic properties of therapeutic proteins.<sup>7</sup> It has been previously reported that PEG-conjugated therapeutic peptides/proteins exhibit clinical properties superior to their corresponding unmodified parental molecules. PEGylation delays drug

absorption, thereby reducing serious side-effects caused by acutely peaking drug concentrations, and also prolongs the half-life of drugs, therefore improving patient compliance by greatly reducing the frequency of drug injections.<sup>8</sup> However, the modification of proteins by PEG via nonselective groups often does not result in homogeneous products. To address this shortcoming, site-directed PEGylation techniques have been developed so that the definite numbers of PEGs could be coupled selectively to proteins. N-terminal residues of the peptide have been proposed as useful selective targets for PEGylation with an advantage of producing homogeneous products without changing the peptide structure.<sup>6</sup> For example, PEG aldehyde derivative such as PEG-butyraldehyde has highly specific affinity to the N-terminal  $\alpha$ -amine of the peptide.<sup>9,10</sup>

In general, PEGylation has been performed with highly purified proteins harvested from inclusion bodies by *in vitro* refolding and purification, followed by multistep purification to attain the desired PEG–protein conjugates. We have provided several pieces of in-depth understanding to the molecular basis of polymer-assisted protein refolding and protein PEGylation.<sup>11–13</sup> Accordingly, we reasoned that the integration of site-specific PEGylation and protein refolding (IPPR) is a

**Received:** July 8, 2013

**Revised:** October 18, 2013

**Published:** December 16, 2013

promising strategy for obtaining modified protein with preserved bioactivity and improved stability directly from inclusion bodies (Figure 1).

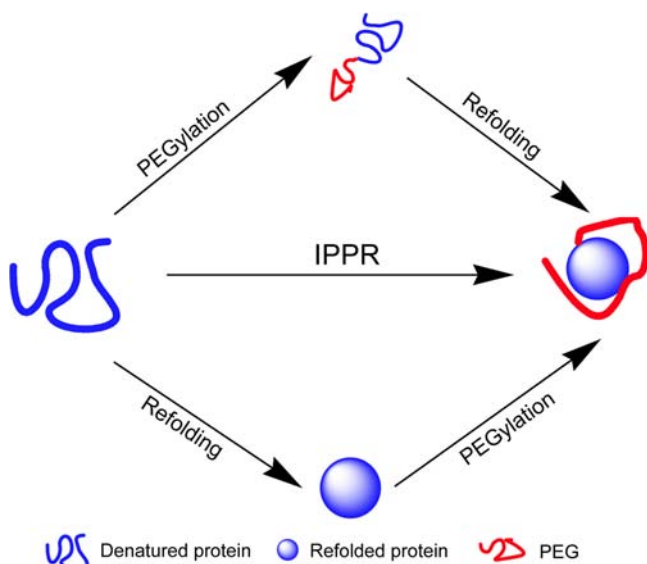


**Figure 1.** Schematic illustration for the integration of PEGylation and refolding (IPPR) of denatured recombinant proteins. Using IPPR, highly purified, site-specific PEGylated proteins, which were successfully refolded, can be obtained directly from inclusion bodies.

In the present study, we investigated the feasibility of IPPR using lysozyme as a model protein. Several different complementary assays, including reverse phase HPLC (RP-HPLC), ion exchange chromatography (IEC), and SDS-PAGE, were used to examine whether PEG-conjugated refolded lysozyme can be obtained by mixing mPEG20kD-butyraldehyde with denatured lysozyme in a protein refolding buffer. RP-HPLC and IEC were used to monitor the IPPR reaction at specific time-points and examined whether PEGylation and protein refolding were performed simultaneously. Subsequently, we used this novel IPPR approach to refold and modify the recombinant human FGF21 (rhFGF21) protein at its N-terminal residues, with mPEG20kD-butyraldehyde. The rhFGF21 protein is an important endocrine regulator of glucose and lipid metabolism<sup>14</sup> and is usually expressed in inclusion bodies in *E. coli*. Our bioactivity and circular dichroism (CD) analyses showed that IPPR-PEGylated rhFGF21 is comparable to the native rhFGF21 protein. In addition, we also applied *in vitro* and *in vivo* biostability analyses to examine whether IPPR-PEGylated rhFGF21 is more stable than non-PEGylated rhFGF21, which allowed for a significantly longer effect on lowering blood glucose and lipid levels in the ob/ob diabetic mouse model.

## EXPERIMENTAL PROCEDURES

**Reagents.** *Pyrobest* DNA Polymerase and restriction enzymes, *Nde*I and *Hind*III, were purchased from TaKaRa Company (Japan). PCR purification, gel extraction, and plasmid miniprep kits were obtained from Promega Company (Madison, WI, USA). Isopropyl-1-thio- $\beta$ -D-galactopyranoside (IPTG) was purchased from Gold BioTechnology (St. Louis, MO, USA). Hen egg white lysozyme, mPEG20 kDa-butyraldehyde (mPEG20K), reduced and oxidized glutathione (GSH and GSSG), dithiothreitol (DTT), urea, and *Micrococcus*

*lysodeikticus* were purchased from Sigma-Aldrich (St. Louis, MO, USA). Anti-hFGF21 antibody was purchased from Santa Cruz Biotechnology Inc. (Santa Cruz, CA, USA). Bradford protein assay reagents used for quantitative protein analysis were purchased from Bio-Rad (Hercules, CA, USA). All chemicals were analytical grade.

**Expression of Insoluble rhFGF21.** DNA coding for human FGF21 was PCR amplified. Following *Nco*I and *Hind*III digestion, PCR fragments were subcloned into a pET bacterial expression vector and the recombinant vector used to transform bacterial host BL21 (DE3) cells. Next, BL21 (DE3) cells were incubated at 37 °C in Luria–Bertani medium containing ampicillin (50  $\mu$ g/mL) until the cell density reached an OD<sub>600</sub> of 0.6. The cells were then incubated at 30 °C and 1.0 mM IPTG added to the medium to induce recombinant product expression. After incubation for 3–4 h, bacteria were collected by centrifugation and the cell pellet was resuspended in 25 mM Tris-HCl (pH 7.5), 1 mM EDTA, 0.6–0.9 M NaCl, and 1 mM phenylmethylsulfonyl fluoride. Cells were lysed by sonication and separated by centrifugation.

**Protein Denaturation–Reduction.** Lysozymes and rhFGF21 inclusion bodies were denatured by incubating 25 mg of proteins in 2.5 mL denaturing buffer (20 mM PB, 8 M urea, 100 mM dithiothreitol, pH 7.0) for 3 h at room temperature, forming a final denatured reduced protein concentration of 10 mg/mL. Complete denaturation of proteins was confirmed by RP-HPLC (Agilent Technologies, Palo Alto, CA).

**IPPR of Lysozyme and rhFGF21.** Each denatured protein solution was applied to a PD-10 column (GE Healthcare Life Sciences, Piscataway, NJ, USA) for DTT removal. IPPR was initiated by rapid dilution of the denatured protein solution into refolding buffer (4 mM EDTA, 1 mM GSSG, 10 mM GSH, 1.5 M urea, 100 mM PB, pH 6.0) either in the absence or in the presence of increasing mPEG20K concentrations and 30 mM sodium cyanoborohydride (NaBH<sub>3</sub>CN), to obtain final lysozyme and rhFGF21 concentrations of 1 mg/mL. Samples were incubated for different times (2, 4, 8, 12, or 24 h) at different temperatures (4, 16, or 25 °C) and reactions were terminated by adding 2% (w/v) glycine. The progress of refolding and PEGylation over time was monitored and quantified using 12% SDS-PAGE and RP-HPLC, as described previously.<sup>10</sup>

Additionally, as controls, conventional PEGylation of native lysozyme and native rhFGF21 with mPEG20K were performed at 25 and 4 °C for 8 h in a phosphate buffer (100 mM PB, pH 6.0) in the presence of 10-fold molar ratios of mPEG20K and 30 mM NaBH<sub>3</sub>CN, respectively.

**RP-HPLC Analysis.** RP-HPLC was performed using Agilent 1100 RP-HPLC (Agilent Technologies, Palo Alto, CA) equipped with an automatic injector and a 300SB-C18 column (Agilent Technologies, Palo Alto, CA). The mobile phase comprised two buffers: Buffer A (distilled H<sub>2</sub>O, 0.1% TFA) and Buffer B (acetonitrile, 0.1% TFA). The RP column was first subjected to an isocratic 10% (v/v) acetonitrile–water gradient for 10 min, followed by a 10–70% (v/v) acetonitrile–water gradient over 60 min, at a total solvent flow rate of 1 mL/min. Absorbance was measured at 280 nm using a UV detector. RP-HPLC was used to analyze denatured protein, refolding protein, PEGylated mixture of native protein, and IPPR-PEGylated mixture. Yields of IPPR-PEGylated and overall IPPR-refolded proteins were quantified as the mass ratio of PEGylated proteins and final refolded protein to initial

denatured protein. Protein mass eluted from the RP-HPLC column was measured by peak integration, based on standard curves obtained by calibration using known concentrations of native protein.

Moreover, RP-HPLC profiles obtained at different IPPR reaction times were used to quantitatively determine the refolding and PEGylated yield of proteins. Specifically, elution peaks of RP-HPLC of IPPR reaction at indicated time-points were identified by SDS-PAGE and quantified based on a standard curve obtained by calibration using known concentrations of native protein as described above.

**IEC Analysis and Purification of IPPR-PEGylated Proteins.** Lysozyme reaction mixtures were applied to CM Sepharose fast flow column (1 mL bed volume; GE Healthcare Life Sciences), pre-equilibrated with 15 column volumes (CVs) of binding buffer (20 mM PB, pH 7.0) at a flow rate of 0.5 mL/min. Samples were washed with 10 CVs of binding buffer, and then eluted with elution buffer A (0.2 M NaCl, 20 mM SPB, pH 7.0) and buffer B (1.0 M NaCl, 20 mM SPB, pH 7.0) over 10 CVs.

RhFGF21 reaction mixtures were applied to HiTrap Q Sepharose fast flow column (1 mL bed volume; GE Healthcare Life Sciences), pre-equilibrated with 15 CVs of binding buffer (20 mM Tris-HCl, pH 8.0) at a flow rate of 0.5 mL/min. Samples were washed with 10 CVs of binding buffer, and then eluted with elution buffer A (80 mM NaCl, 20 mM Tris-HCl, pH 8.0) and buffer B (200 mM NaCl, 20 mM Tris-HCl, pH 8.0) over 10 CVs. All elution fractions were collected and analyzed by 12% SDS-PAGE.

**Activity Assays for IPPR-PEGylated Proteins.** *Lysozyme Activity Assay.* The activity of lysozyme and IPPR-PEGylated lysozyme was measured from their bioactivity on *Micrococcus lysodeikticus* (*M. lysodeikticus*), as described previously.<sup>11</sup>

*Cell Culture and Glucose Uptake Experiments for IPPR-PEGylated rhFGF21.* 3T3-L1 preadipocytes (American Type Culture Collection, Rockville, MD, USA) were maintained in DMEM containing 10% fetal bovine serum (Invitrogen, Carlsbad, CA, USA). Adipocyte differentiation was induced by culturing the cells for 2 days in differentiation medium (DMEM with 10% FBS, 10 mM HEPES/MEM, nonessential amino acids (NEAA), penicillin/streptomycin (PC/SM), 2  $\mu$ M insulin, 1  $\mu$ M dexamethasone, 0.25 mM 3-isobutyl-1-methyl-xanthine (IBMX); all from Sigma-Aldrich, St. Louis, MO, USA), and then in differentiation medium without dexamethasone and IBMX for a further 2 days.<sup>14</sup> Thereafter, the medium was changed every 2 days with DMEM supplemented with 10% FBS, 10 mM HEPES, NEAA, and PC/SM. Lipid droplet accumulation was observed in >95% of cells after 7 days, and cells at days 7–10 were used for experiments.

For glucose uptake, cells cultured in multiwell plates were serum-starved overnight and then treated with different concentrations of either native or IPPR rhFGF21 (0.1, 1, 10, and 100 nmol/L) for 24 h. Plates were washed twice with KRP buffer [15 mM HEPES (pH 7.4), 118 mM NaCl, 4.8 mM KCl, 1.2 mM MgSO<sub>4</sub>, 1.3 mM CaCl<sub>2</sub>, 1.2 mM KH<sub>2</sub>PO<sub>4</sub>, 0.1% BSA], and then 100  $\mu$ L of KRP buffer containing 2-deoxy-D-[<sup>14</sup>C]glucose (2-DOG; 0.1  $\mu$ Ci, 100  $\mu$ M) was added to each well. To eliminate nonspecificity, control wells contained 100  $\mu$ L of KRP buffer with 2-DOG (0.1  $\mu$ Ci, 10 mM). Uptake reactions were performed at 37 °C for 1 h, terminated by addition of cytochalasin B (20  $\mu$ M), and measured using a Wallac 1450 MicroBeta counter (Perkin-Elmer, Waltham, MA, USA).

**Mass Spectrometry and N-Terminal Analysis of IPPR-PEGylated rhFGF21.** Mass spectra were acquired using an Applied Biosystems Voyager System DE PRO MALDI-TOF mass spectrometer (Carlsbad, CA, USA) with a nitrogen laser. The matrix was a saturated solution of *R*-cyano-4-hydroxycinnamic acid in a 50:50 mixture of acetonitrile and water containing 0.1% trifluoroacetic acid. Purified IPPR-PEGylated rhFGF21 and matrix were mixed at a ratio of 1:1, and 1  $\mu$ L spotted onto a 100-well sample plate. All spectra were acquired in positive mode, and over the range 600–2500 Da under reflectron conditions (20 kV accelerating voltage, 350 ns extraction delay time), and 2–100 kDa under linear conditions (25 kV accelerating voltage, 750 ns extraction delay time). The N-terminal amino acid sequence of IPPR-PEGylated rhFGF21 was examined using the Edman degradation method,<sup>15</sup> followed by MALDI-TOF mass spectroscopy as described above.

**Circular Dichroism Spectroscopy Analysis.** Secondary structures of native and IPPR-PEGylated rhFGF21 were determined using a CD spectropolarimeter (Model J-810; Jasco, Japan). Far-UV CD spectra were recorded at wavelengths between 190 and 250 nm using a 0.1 cm path length cell at 25 °C with a protein concentration of 6  $\mu$ M in 10 mM PBS, pH 7.0. Each spectrum was obtained from an average of six scans, and CD spectra were corrected for buffer contributions. CD data were presented as a function of wavelength, in terms of the mean residue ellipticity. The thermodynamic stability of IPPR-PEGylated rhFGF21 was also determined by CD spectroscopy. In thermal stability experiments, the protein solution was heated with a temperature gradient of 20–60 °C, and protein conformation changes monitored by CD spectroscopy as described above.

**Functional Evaluation of IPPR-PEGylated rhFGF21.** *Animal Models.* Adult (aged 11–12 weeks) obese *Lep<sup>ob/ob</sup>* C57BL/6 (*ob/ob*) mice and normal control C57BL/6 mice (aged 8–12 weeks) were purchased from the Model Animal Research Center of Nanjing University, China. All mice were housed in a temperature-controlled environment with a 12 h light/dark cycle, free access to water, and a standard chow diet containing 60% carbohydrate, 13% fat, and 27% protein on a caloric basis. Animal care and experiments were followed the Guide for the Care and Use of Laboratory Animals provided by U.S. National Institutes of Health and were approved by the Animal Care and Use Committee of Wenzhou Medical University, China. The *ob/ob* mice were randomly divided into three groups (*n* = 9): two groups of mice were treated either with 20 nmol/kg IPPR-rhFGF21 or with 20 nmol/kg native rhFGF21 and one group were treated with 0.9% physiological saline as positive sham. In addition, normal control C57BL/6 mice treated with 0.9% physiological saline (*n* = 9) were used as negative sham. IPPR-PEGylated and native rhFGF21 were given once a day for 1 week via subcutaneous injection.

**Antidiabetic Effects of IPPR-PEGylated rhFGF21.** On days 4 and 7 after treatment, animals were tail bled (by tail snip) 1 h after the last injection of physiological saline, native, or IPPR-PEGylated rhFGF21. Glucose and plasma triglyceride levels were determined using the Precision G Blood Glucose Testing System (Abbott Laboratories, Abbott Park, IL, USA) and the Hitachi 912 Clinical Chemistry Analyzer (Roche Diagnostics, Indianapolis, IN, USA), respectively. In addition, the long-lasting antidiabetic effect of rhFGF21 was also compared by examining plasma glucose and triglyceride levels in *ob/ob* mice

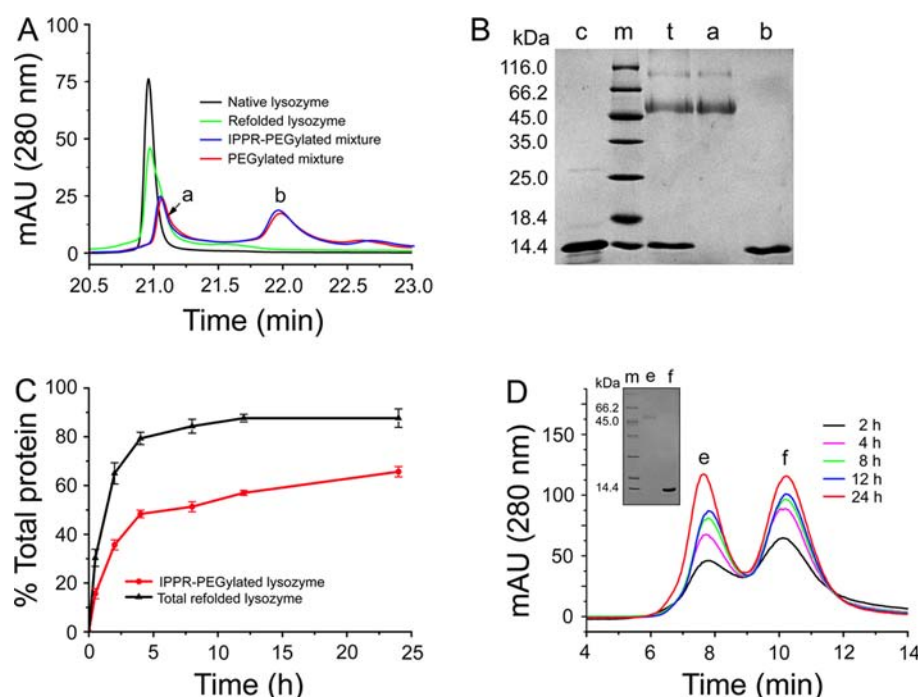


**Figure 2.** Determining IPPR feasibility using lysozyme as a model protein. (A) RP-HPLC analysis of native, refolded, PEGylated native, and IPPR-PEGylated lysozyme. (B) SDS-PAGE analysis of RP-HPLC fractions. Lane c, native lysozyme; lane m, molecular weight standards; lane t, IPPR reaction mixture; lane a, eluted fraction (IPPR) of Peak A from RP-HPLC; lane b, eluted fraction (IPPR) of Peak B from RP-HPLC. (C) Yields of IPPR-PEGylated and overall IPPR refolded lysozyme at different time-points. Yields were calculated from RP-HPLC relative peak areas, based on the standard calibration curve. (D) Elution chromatogram, from CM Sepharose fast flow column, of the IPPR mixture which obtained at different reaction times. Insert panel. SDS-PAGE analysis of fractions collected from CM Sepharose fast flow column. Lane m, molecular weight standards; lane e, eluted fraction (IPPR) of Peak e from IEC; lane f, eluted fraction (IPPR) of Peak f from IEC.

at 4 and 7 days after cessation of a 1-week treatment with native or IPPR-PEGylated rhFGF21. At the end of the study (day 7 after treatment cessation), all ob/ob mice were sacrificed and liver tissues were fixed in 10% zinc-formalin for processing, embedding with paraffin, sectioning at a thickness of 5  $\mu$ m, and staining with hematoxylin-eosin (HE), as described previously.<sup>16</sup>

**Protein Concentration.** Protein concentrations were measured using the Bradford method with BSA as the protein standard.<sup>17</sup>

**Statistical Analysis.** For cell-based studies, data were collected from three independent experiments, and for *in vivo* studies, nine rats used per group. Results are expressed as mean  $\pm$  standard deviation. One-way ANOVA followed by a post hoc Turkey's test was used for determining statistical differences between groups. Statistical tests were performed using Origin 7.5 laboratory data analysis and graphing software. *P* values <0.05 or 0.01 were considered statistically significant.

## RESULTS

**Determining the Feasibility of IPPR Using Lysozyme as a Model Protein.** In order to determine if protein refolding and PEGylation can occur simultaneously in the chosen refolding buffer (described in Experimental Procedures), chemically denatured lysozyme (1 mg/mL) was refolded in the presence of mPEG20K (5 mg/mL) for designated reaction times. The reaction mixture was analyzed by RP-HPLC, with elution fractions identified by SDS-PAGE and then subsequently quantitated by RP-HPLC. As shown in Figure 2A, when the reaction samples were incubated for 12 h at 25  $^{\circ}$ C, IPPR-PEGylated lysozyme had the same retention time as

PEGylated lysozyme, obtained from a conventional PEGylation approach with native lysozyme, and the retention time of non-PEGylated refolded lysozyme was identical to native lysozyme. SDS-PAGE analysis of IPPR fractions, eluted from RP-HPLC columns, showed refolded lysozyme was conjugated to a single mPEG20kD molecule (Figure 2B). Additionally, RP-HPLC profiles obtained at different IPPR reaction times were used to quantitatively determine, based on protein mass quantification, the refolding yield, and PEGylated efficiency of lysozyme. The amount of IPPR and overall refolded lysozyme at specific reaction time-points during IPPR are shown in Figure 2C, the yield of IPPR lysozyme increased accompanied by an enhancement of refolding yield, which was also confirmed by IEC (Figure 2D). Table 1 summarizes the enzymatic activities

**Table 1. Enzymatic Activity of Different Forms of Lysozyme**

	relative activity
native lysozyme	100%
unfolded lysozyme	0%
refolded lysozyme	89%
PEGylated native lysozyme	5%
IPPR-PEGylated lysozyme	5%

of native, unfolded, refolded, and PEGylated lysozyme forms. Importantly, the enzymatic activity of IPPR-PEGylated lysozyme was exactly similar to PEGylated native lysozyme, indicating that IPPR had no detrimental effect on protein. Additionally, the PEGylated lysozyme showed significantly reduced enzymatic activity compared with the unmodified

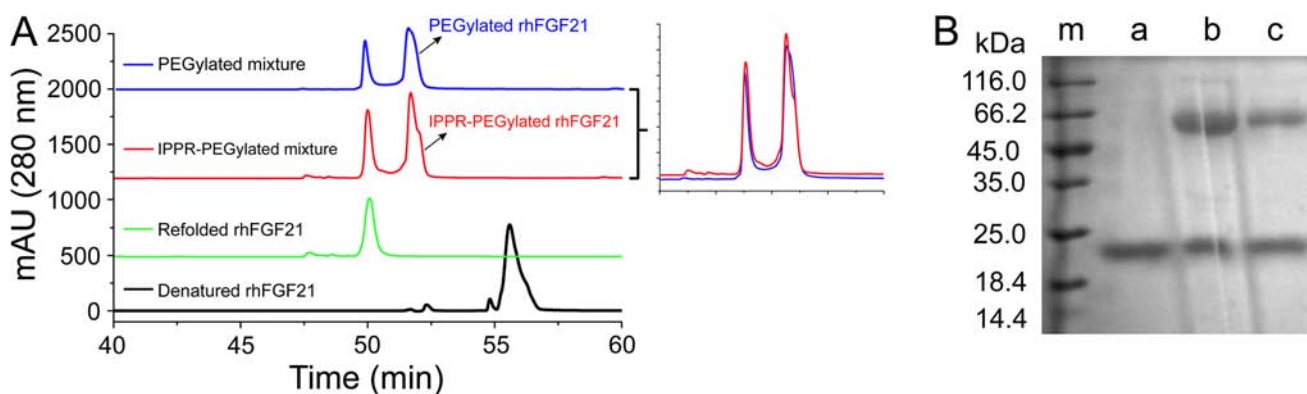


**Figure 3.** IPPR of denatured rhFGF21. (A) RP-HPLC analysis of denatured rhFGF21, refolded rhFGF21, PEGylated products of native rhFGF21, and IPPR-PEGylated products of refolded rhFGF21 obtained at a PEG-to-protein ratio of 10:1, reaction time of 8 h, reaction temperature of 4 °C, and pH of 6.0, respectively. Superimposition of RP-HPLC profiles of PEGylated products of native rhFGF21 and IPPR-PEGylated products of refolded rhFGF21 (insert panel). (B) SDS-PAGE analysis of IPPR-PEGylated and conventionally PEGylated products. Lane M, molecular weight standards; lane a, native rhFGF21; lanes b and c, IPPR-PEGylated and conventional PEGylated products.

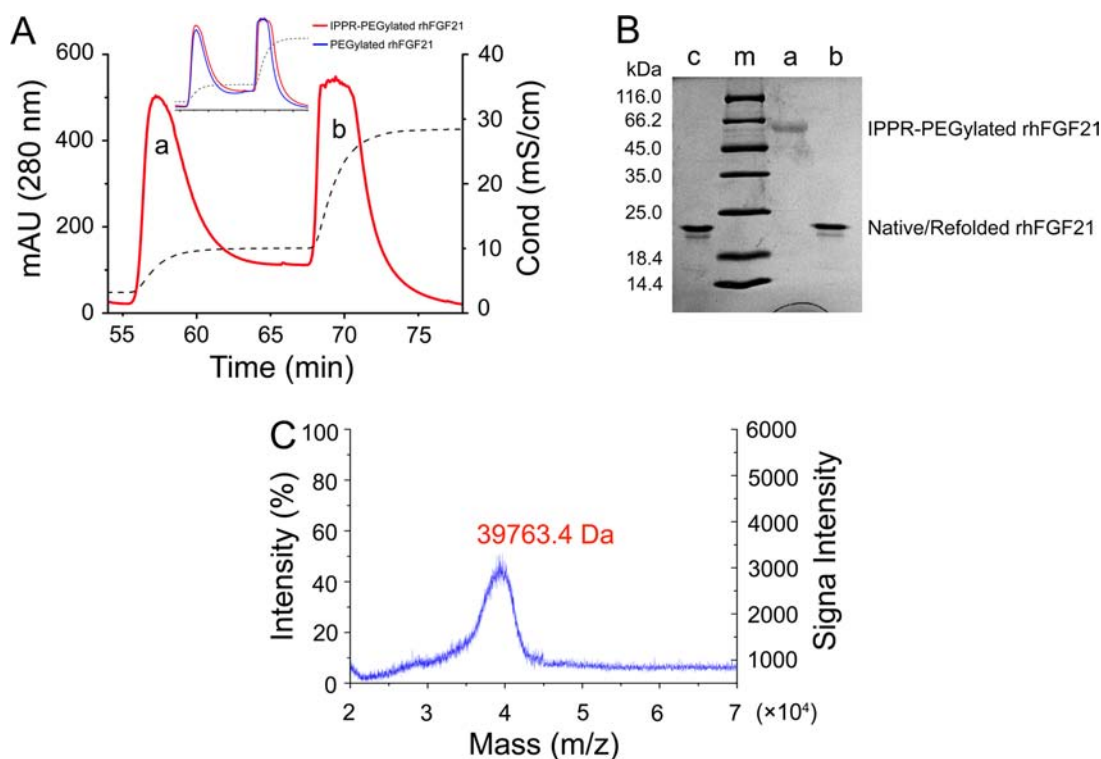


**Figure 4.** Purification and validation of IPPR-PEGylated rhFGF21. (A) Elution profile of the IPPR mixture from HiTrap Q Sepharose fast flow column. Comparison of elution profiles of PEGylated native rhFGF21 and IPPR-PEGylated rhFGF21 (insert panel). (B) SDS-PAGE analysis of fractions collected from HiTrap Q Sepharose fast flow column. Lane c, native rhFGF21; lane m, molecular weight standards; lane a, eluted fraction (IPPR) of Peak a from IEC; lane b, eluted fraction (IPPR) of Peak b from IEC. (C) Molecular mass determination of IPPR-PEGylated rhFGF21 (39 763 Da) using MALDI-TOF mass spectrometry.

enzyme, because PEGylation had adverse effect on lysozyme bioactivity as previously documented.<sup>9</sup>

**IPPR Application for rhFGF21.** To determine optimal conditions for IPPR of denatured rhFGF21, the effects of different PEG/protein molar ratios (ranging from 1/1 to 20/1), reaction times (2, 4, 8, 12, or 24 h) and temperatures (4, 16, or 25 °C), on the yield and efficiency of site-specific mono-PEGylation were examined. We found the optimal yield of mono-PEGylated refolded rhFGF21 was achieved when the reaction was performed under the following conditions: denatured rhFGF21 was diluted 10 times into refolding buffer (4 mM EDTA, 1 mM GSSG, 10 mM GSH, 1.5 M urea, 100

mM PB, pH 6.0) to a final protein concentration of 1 mg/mL, in the presence of 10-fold molar ratios of mPEG20K and 30 mM NaBH<sub>3</sub>CN, at 4 °C for 8 h. Under optimal conditions, RP-HPLC and SDS-PAGE analysis showed 59.3% of total rhFGF21 was successfully mono-PEGylated (Figure 3A,B). In parallel, we compared the modification efficiency of IPPR with conventional PEGylation, which was performed using native rhFGF21. Under the optimized IPPR conditions, the PEGylated yield of native rhFGF21 was 61.2%, similar to levels obtained by IPPR (Figure 3A,B). Additionally, both RP-HPLC and IEC behaviors of IPPR-refolded and IPPR-PEGylated rhFGF21 were consistent with non-PEGylated and

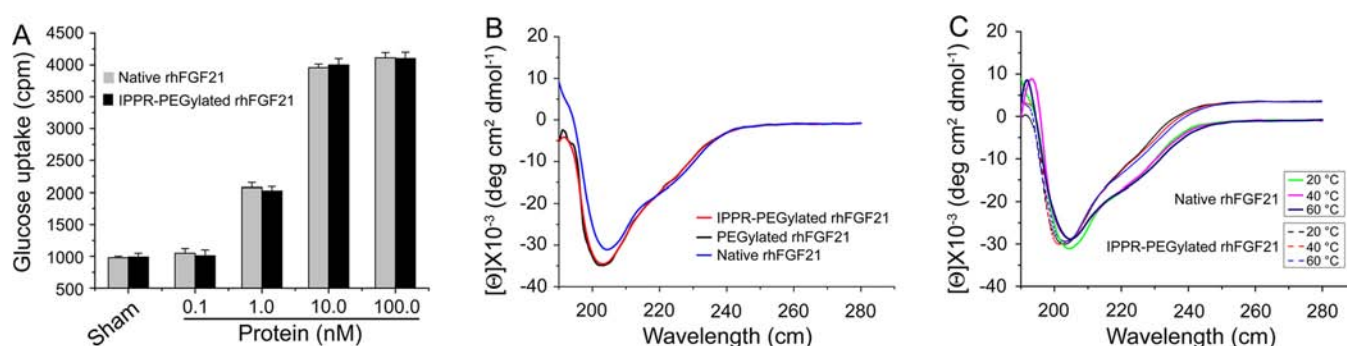


**Figure 5.** Examination of the bioactivity and structural integrity of IPPR-PEGylated rhFGF21. (A) Cellular glucose uptake stimulated by native and IPPR-PEGylated rhFGF21 in 3T3-L1 cells. Values ( $\pm$ SEM) are the average of at least three independent measurements. (B) Far-UV CD spectra of native, PEGylated native, and IPPR-PEGylated rhFGF21. (C) Thermal stability comparison of native and IPPR-PEGylated rhFGF21, heated with temperature gradients ranging from 20 to 60 °C. Protein conformation changes were monitored by CD spectroscopy.

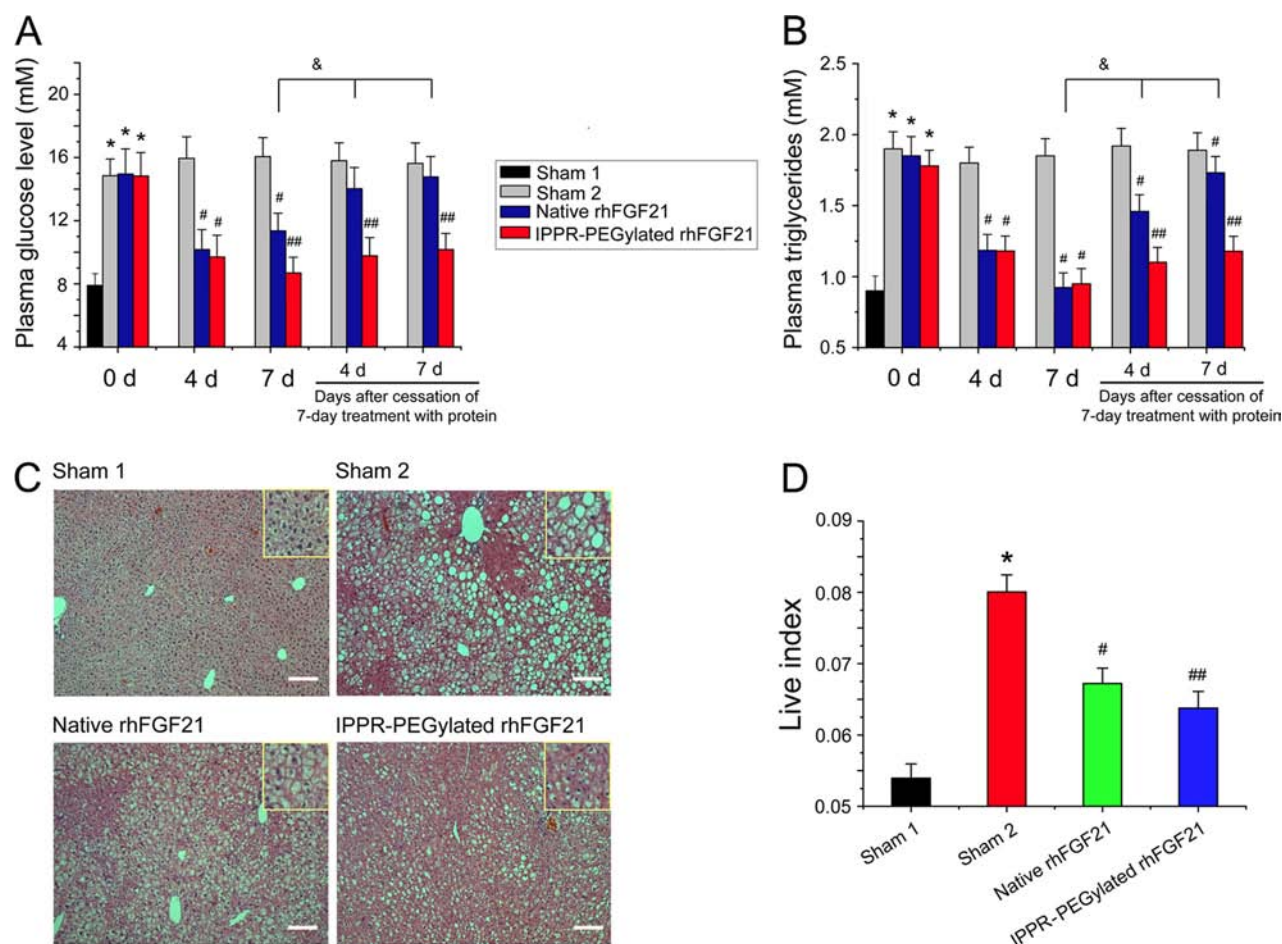


**Figure 6.** Therapeutic effect of IPPR-PEGylated rhFGF21 in the ob/ob mouse model. (A,B) Effect of IPPR-PEGylated rhFGF21 on plasma glucose and triglyceride levels. Animals were treated (via subcutaneous injection) with IPPR-PEGylated and native rhFGF21 once a day for 1 week. On days 4 and 7, glucose (A) and plasma triglyceride (B) levels were determined. In addition, the long-lasting antidiabetic effects of the two rhFGF21 forms were compared by examining plasma glucose (A) and triglyceride (B) levels of days 4 and 7 after cessation of 7-day treatment with native or IPPR-PEGylated rhFGF21. \*  $p < 0.01$  vs sham 1 (negative sham, normal C57BL/6 mice treated with vehicle); #  $p < 0.05$  vs sham 2 (positive sham, ob/ob mice treated with vehicle); ##  $p < 0.05$  vs corresponding native rhFGF21; &  $p < 0.01$  vs corresponding 7-day treatment. (C,D) Changes in fat droplet intensity (C) and liver index (liver weight/total body weight) (D) from liver sections of ob/ob mice, on days 7 after treatment cessation with native or IPPR-PEGylated rhFGF21. \*  $p < 0.01$  vs sham 1; #  $p < 0.01$  vs sham 2; ##  $p < 0.05$  vs corresponding native rhFGF21.

PEGylated native rhFGF21, respectively (Figures 3A and 4A), indicating that denatured rhFGF21 was successfully refolded and PEGylated by IPPR.

**Purification and Validation of IPPR-PEGylated rhFGF21.** To purify IPPR-PEGylated rhFGF21, IPPR reaction

mixtures were subjected to salt gradient cation-exchange chromatography on a HiTrap Q Sepharose fast flow column. After cation-exchange chromatography, IPPR-PEGylated and non-PEGylated rhFGF21 were eluted in two separate peaks, as confirmed by SDS-PAGE (Figure 4A,B). To verify that IPPR-

PEGylated rhFGF21 was mono-PEGylated, MALDI-TOF mass spectrometry (MALDI-TOF-MS) was employed. Our MS data showed IPPR-PEGylated rhFGF21 had a molecular weight of 39.76 kDa (Figure 4C), confirming that a single 20kD PEG molecule was conjugated to rhFGF21 (MW: 19.42 kDa).<sup>12,18</sup> The broad MS peak corresponding to IPPR-PEGylated rhFGF21 was most likely due to PEG polydispersity, as reported previously.<sup>10</sup> Next, we used automated N-terminal sequencing by Edman degradation to determine the IPPR-PEGylated site on refolded rhFGF21. Using this method of sequencing, the five N-terminal amino acids (His-Pro-Ile-Pro-Asp) were detected in non-PEGylated rhFGF21 only (data not shown). The N-terminal residues of IPPR-PEGylated rhFGF21 were not detected, suggesting covalent attachment of PEG to the N-terminal  $\alpha$ -amino group does not allow the N-terminal Ser residue to be modified by 1-fluoro-2,4-dinitrobenzene in the sequencing reaction, therefore making it unrecoverable.<sup>15</sup> Taken together, the MS and sequencing data unambiguously confirmed that a PEG molecule was site-directly attached to the N-terminus of rhFGF21 by IPPR-PEGylation.

**Analysis of Bioactivity of IPPR-PEGylated rhFGF21.** To evaluate the bioactivity of IPPR-PEGylated rhFGF21, its effect on glucose uptake in differentiated mouse 3T3-L1 adipocytes<sup>14</sup> was compared with non-PEGylated native rhFGF21. As shown in Figure 5A, IPPR-PEGylated rhFGF21 and native rhFGF21 induced a comparable response on enhancing glucose uptake in 3T3-L1 adipocytes, further demonstrating that denatured rhFGF21 was correctly refolded by IPPR and there was no adverse effect of IPPR on rhFGF21 bioactivity.

**Effect of IPPR on the Structural Integrity and Stability of rhFGF21.** To investigate the effect of IPPR on rhFGF21 structure, the secondary structure of IPPR-PEGylated rhFGF21 was compared with native rhFGF21 using CD spectroscopy. Far-UV CD spectra recorded for IPPR-PEGylated rhFGF21 was comparable to non-PEGylated native rhFGF21 (Figure 5B), demonstrating that IPPR aided protein refolding and did not alter the secondary structure of rhFGF21.

PEGylation has been shown to stabilize protein structures while also making their activities substantially more robust, with respect to temperature changes.<sup>19</sup> The thermal stability of native and IPPR-PEGylated rhFGF21 was compared by incubating the proteins in temperature gradients ranging from 20 to 60 °C, and monitoring any protein conformation changes or heat effects by CD spectroscopy. Far UV-CD spectra showed native rhFGF21 had a disordered structure when the temperature was increased from 20 to 40 °C (or higher), as determined from its large negative ellipticity around 200 nm and its low ellipticity at 190 nm (Figure 5C). In contrast, the secondary structure of IPPR-PEGylated rhFGF21 was minimally impacted in the thermostability assay.

**Antidiabetic Effects of IPPR-PEGylated rhFGF21 in ob/ob Mice.** The preserved function and increased thermostability of IPPR-PEGylated rhFGF21 promoted us to determine whether the modified protein could provide similar or even better therapeutic effect on diabetes *in vivo* as or than the native rhFGF21. We administered both rhFGF21 forms to ob/ob mice, a mouse model of hyperglycemia and insulin resistance.<sup>20</sup> Our results demonstrated that 4-day treatment with both native and IPPR-PEGylated rhFGF21 significantly lowered blood glucose, and this effect on 7-day treatment was even more pronounced (Figure 6A). Similarly, the triglyceride-lowering effect was also evident for IPPR-PEGylated rhFGF21 treatment in ob/ob mice (Figure 6B). Moreover, compared with the

native rhFGF21 on days 7 of the treatment, IPPR-PEGylated rhFGF21 produced an observable improvement in the hypoglycemic effect (Figure 6A). The improved hypoglycemic effect of IPPR-PEGylated rhFGF21 may be due to the increase in its *in vivo* biostability.

To test this above assumption, we examined plasma glucose and triglyceride levels at different times (immediately (0), 4 days, and 7 days) after cessation of 7-day treatment with native or IPPR-PEGylated rhFGF21. Plasma glucose and triglyceride levels gradually returned to approximately vehicle control levels in ob/ob mice treated with native rhFGF21, but remained at significantly low levels in mice treated with IPPR-PEGylated rhFGF21 (Figure 6A,B).

In previous studies, systemic rhFGF21 was reported to significantly reverse hepatic steatosis and decrease tissue lipid contents in the type 2 diabetic animal model.<sup>21</sup> Therefore, we examined liver tissues on days 7 after cessation of 7-day treatment with either native or IPPR-PEGylated rhFGF21. Histological examination for the liver sections of ob/ob mice treated with native rhFGF21 (Figure 6C) showed the extensive existence of micro- and macrovesicular hepatocyte vacuolation, reflecting intrahepatic fat accumulation. In contrast, hepatocellular vacuolation and lipid droplets were significantly reduced in the liver sections of ob/ob mice treated with IPPR-PEGylated rhFGF21, even on days 7 after treatment cessation (Figure 6C), consistent with liver weight indexes (Figure 6D). These results strongly support our hypothesis that (1) denatured rhFGF21 can be correctly refolded by IPPR; and (2) improved *in vivo* biostability of the IPPR-PEGylated rhFGF21 provides a significantly and long-lasting antidiabetic effect, compared with the native rhFGF21.

## DISCUSSION

Recombinant proteins in bacteria, such as *E. coli* are often expressed in the form of inclusion bodies inside the cells.<sup>1</sup> To recover bioactive forms of expressed protein from *E. coli* inclusion bodies, a multistep, delicate refolding process is required. The process usually consists of *in vitro* refolding and purification steps,<sup>22</sup> although even after recovery of the refolded protein other common problems are encountered, for example, poor stability and relatively short half-life *in vivo*,<sup>14,23,24</sup> which have restricted their potential clinical applications. Surface modifications, such as PEGylation of therapeutic proteins, are widely studied as a means to improve in-serum circulation stability and reduce immunogenicity.<sup>13,25,26</sup> Combining PEGylation with a refolding process to obtain bioactive and PEGylated proteins directly from inclusion bodies (i.e., IPPR) would significantly improve downstream processing performance. Additionally, the efficiency of this process may be drastically improved by simplifying the conventional steps of inclusion body refolding, purification of refolded protein, PEGylation, and purification of PEGylated protein.

In the present study, we sought to determine the feasibility of IPPR, first using denatured lysozyme as a model protein for PEGylation under specific refolding conditions. IPPR-refolded and IPPR-PEGylated lysozyme, representing non-PEGylated and conventionally PEGylated native protein, respectively, exhibit comparable hydrophobic and structural characteristics. It is encouraging that we have shown PEGylation and refolding can be performed simultaneously under the correct lysozyme refolding conditions, which is different from the previous study did by Minyoung Kim and his colleague.<sup>27</sup> In their study, lipase was used as a model protein for PEGylation under a reducing

and denaturing condition and then *in vitro* refolding of PEGylated protein was performed by a traditional 'dilution' method.

We also extended our novel IPPR method to rhFGF21, which is an attractive candidate for the potential treatment of human type 2 diabetes and associated metabolic syndrome.<sup>14,28</sup> Until now, rhFGF21 was mostly produced in *E. coli*-expression systems within inclusion bodies. The *in vitro* stability and *in vivo* half-life of rhFGF21 are short, and the immunogenic activity is high,<sup>14</sup> all properties that have strongly restricted its clinical applications. Denatured rhFGF21 was successfully refolded and mono-PEGylated by IPPR under the determined optimal reaction conditions. Although it has already been reported that N-terminal  $\alpha$ -amine of proteins is highly amenable for site-specific modifications,<sup>29,30</sup> our current study extends this knowledge to proteins which are insoluble, expanding the potential application to a vast number of protein therapeutics.

Theoretically, as an alternative downstream processing technique, IPPR should not affect the folding or the intracellular action of proteins (Figure SA,B). The increased thermostability of PEGylated protein species further demonstrates its appealing application (Figure 5C). Changes in CD spectroscopy observed at elevated temperatures (20 to 60 °C) may be explained by reduced thermodynamic stability of the protein structure and increased hydrophobic interactions from exposed hydrophobic patches;<sup>19,30</sup> therefore, conjugated PEG may "swim around" the hydrophobic rhFGF21 patches to suppress hydrophobic interactions.<sup>12</sup>

More importantly, our physiological results suggested that IPPR-PEGylated rhFGF21 can sustainably lower blood glucose and triglyceride levels in the ob/ob mouse model. We found both plasma glucose and triglyceride levels in IPPR-PEGylated rhFGF21 treatment group were 40% lower than those in native rhFGF21-treated diabetic rats on days 7 after cessation of 7-day treatment (Figure 6A,B). In addition, hepatocellular vacuolation and lipid droplets were significantly reduced in the liver sections from ob/ob mice, even on days 7 after treatment cessation (Figure 6C,D). This clearly demonstrated that denatured rhFGF21 was successfully refolded and IPPR-PEGylation can enhance rhFGF21 function *in vivo* by sustaining antidiabetic effects in ob/ob mice for approximately 1 week without additional treatment. Thus, IPPR-PEGylated rhFGF21 shows favorable parameters for clinical application as it requires less frequent administration.

In conclusion, IPPR offers a one-step facile approach for high yield production of bioactive proteins. Importantly, IPPR is both time- and cost-effective compared to existing methodologies and hence will have a major impact on the drug development arena by facilitating the manufacturing of protein therapeutics for use in variety of human diseases.

## AUTHOR INFORMATION

### Corresponding Authors

\*Tel.: +86 13645770691; fax: +86 577 86689983; E-mail address: nyuhuang@gmail.com.

\*Tel.: +86 13540609283; fax: +86 028 85260436; E-mail address: liubl@cioc.ac.cn.

### Notes

The authors declare no competing financial interest.

## ACKNOWLEDGMENTS

The authors are thankful to Dr. Moosa Mohammadi and Belov Artur for critically reading the manuscript and making thoughtful suggestions. This work was supported by grants from the Natural Science Foundation of China (81102486 to Z.H. and 81273421 to H.W.); Zhejiang Key Group Project in Scientific Innovation (2010R10042-01 to Z.H.); and Science grant of Wenzhou Department of Science and Technology (Y20090016 to Y.Z.).

## REFERENCES

- (1) Baneyx, F., and Mujacic, M. (2004) Recombinant protein folding and misfolding in *Escherichia coli*. *Nat. Biotechnol.* 22, 1399–408.
- (2) Gautam, S., Dubey, P., Singh, P., Kesavardhana, S., Varadarajan, R., and Gupta, M. N. (2012) Smart polymer mediated purification and recovery of active proteins from inclusion bodies. *J. Chromatogr., A* 1235, 10–25.
- (3) Goldberg, M. E., Rudolph, R., and Jaenicke, R. (1991) A kinetic study of the competition between renaturation and aggregation during the refolding of denatured-reduced egg white lysozyme. *Biochemistry* 30, 2790–7.
- (4) Yamaguchi, S., Yamamoto, E., Mannen, T., and Nagamune, T. (2013) Protein refolding using chemical refolding additives. *Biotechnol. J.* 8.
- (5) Cleland, J. L., Hedgepeth, C., and Wang, D. I. (1992) Polyethylene glycol enhanced refolding of bovine carbonic anhydrase B. Reaction stoichiometry and refolding model. *J. Biol. Chem.* 267, 13327–34.
- (6) Roberts, M. J., Bentley, M. D., and Harris, J. M. (2002) Chemistry for peptide and protein PEGylation. *Adv. Drug Delivery Rev.* 54, 459–76.
- (7) Caliceti, P., and Veronese, F. M. (2003) Pharmacokinetic and biodistribution properties of poly(ethylene glycol)-protein conjugates. *Adv. Drug Delivery Rev.* 55, 1261–77.
- (8) Fishburn, C. S. (2008) The pharmacology of PEGylation: balancing PD with PK to generate novel therapeutics. *J. Pharm. Sci.* 97, 4167–83.
- (9) Shang, X., Yu, D., and Ghosh, R. (2011) Integrated solid-phase synthesis and purification of PEGylated protein. *Biomacromolecules* 12, 2772–9.
- (10) Lee, B. K., Kwon, J. S., Kim, H. J., Yamamoto, S., and Lee, E. K. (2007) Solid-phase PEGylation of recombinant interferon alpha-2a for site-specific modification: process performance, characterization, and *in vitro* bioactivity. *Bioconjugate Chem.* 18, 1728–34.
- (11) Ye, C., Ilghari, D., Niu, J., Xie, Y., Wang, Y., Wang, C., Li, X., Liu, B., and Huang, Z. (2012) A comprehensive structure-function analysis shed a new light on molecular mechanism by which a novel smart copolymer, NY-3–1, assists protein refolding. *J. Biotechnol.* 160, 169–75.
- (12) Huang, Z., Wang, H., Lu, M., Sun, C., Wu, X., Tan, Y., Ye, C., Zhu, G., Wang, X., Cai, L., and Li, X. (2011) A better anti-diabetic recombinant human fibroblast growth factor 21 (rhFGF21) modified with polyethylene glycol. *PLoS One* 6, e20669.
- (13) Huang, Z., Ye, C., Liu, Z., Wang, X., Chen, H., Liu, Y., Tang, L., Zhao, H., Wang, J., Feng, W., and Li, X. (2012) Solid-phase N-terminus PEGylation of recombinant human fibroblast growth factor 2 on heparin-sepharose column. *Bioconjugate Chem.* 23, 740–50.
- (14) Kharitononkov, A., Shiyanova, T. L., Koester, A., Ford, A. M., Micanovic, R., Galbreath, E. J., Sandusky, G. E., Hammond, L. J., Moyers, J. S., Owens, R. A., Gromada, J., Brozinick, J. T., Hawkins, E. D., Wroblewski, V. J., Li, D. S., Mehrbod, F., Jaskunas, S. R., and Shanafelt, A. B. (2005) FGF-21 as a novel metabolic regulator. *J. Clin. Invest.* 115, 1627–35.
- (15) Guerra, P. I., Acklin, C., Kosky, A. A., Davis, J. M., Treuheit, M. J., and Brems, D. N. (1998) PEGylation prevents the N-terminal degradation of megakaryocyte growth and development factor. *Pharm. Res.* 15, 1822–7.

- (16) Hotta, Y., Nakamura, H., Konishi, M., Murata, Y., Takagi, H., Matsumura, S., Inoue, K., Fushiki, T., and Itoh, N. (2009) Fibroblast growth factor 21 regulates lipolysis in white adipose tissue but is not required for ketogenesis and triglyceride clearance in liver. *Endocrinology* 150, 4625–33.
- (17) Bradford, M. M. (1976) A rapid and sensitive method for the quantitation of microgram quantities of protein utilizing the principle of protein-dye binding. *Anal. Biochem.* 72, 248–54.
- (18) Wang, H., Xiao, Y., Fu, L., Zhao, H., Zhang, Y., Wan, X., Qin, Y., Huang, Y., Gao, H., and Li, X. (2010) High-level expression and purification of soluble recombinant FGF21 protein by SUMO fusion in *Escherichia coli*. *BMC Biotechnol.* 10, 14.
- (19) Manning, M. C., Chou, D. K., Murphy, B. M., Payne, R. W., and Katayama, D. S. (2010) Stability of protein pharmaceuticals: an update. *Pharm. Res.* 27, 544–75.
- (20) Kennedy, A. J., Ellacott, K. L., King, V. L., and Hasty, A. H. (2010) Mouse models of the metabolic syndrome. *Dis. Models & Mech.* 3, 156–66.
- (21) Xu, J., Lloyd, D. J., Hale, C., Stanislaus, S., Chen, M., Sivits, G., Vonderfecht, S., Hecht, R., Li, Y. S., Lindberg, R. A., Chen, J. L., Jung, D. Y., Zhang, Z., Ko, H. J., Kim, J. K., and Veniant, M. M. (2009) Fibroblast growth factor 21 reverses hepatic steatosis, increases energy expenditure, and improves insulin sensitivity in diet-induced obese mice. *Diabetes* 58, 250–9.
- (22) Mollania, N., Khajeh, K., Ranjbar, B., Rashno, F., Akbari, N., and Fathi-Roudsari, M. (2013) An efficient in vitro refolding of recombinant bacterial laccase in *Escherichia coli*. *Enzyme Microb. Technol.* 52, 325–30.
- (23) Chen, B. L., and Arakawa, T. (1996) Stabilization of recombinant human keratinocyte growth factor by osmolytes and salts. *J. Pharm. Sci.* 85, 419–26.
- (24) Nguyen, T. H., Kim, S. H., Decker, C. G., Wong, D. Y., Loo, J. A., and Maynard, H. D. (2013) A heparin-mimicking polymer conjugate stabilizes basic fibroblast growth factor. *Nat. Chem.* 5, 221–7.
- (25) Huang, Z., Ni, C., Chu, Y., Wang, S., Yang, S., Wu, X., Wang, X., Li, X., Feng, W., and Lin, S. (2009) Chemical modification of recombinant human keratinocyte growth factor 2 with polyethylene glycol improves biostability and reduces animal immunogenicity. *J. Biotechnol.* 142, 242–9.
- (26) Gong, N., Ma, A. N., Zhang, L. J., Luo, X. S., Zhang, Y. H., Xu, M., and Wang, Y. X. (2011) Site-specific PEGylation of exenatide analogues markedly improved their glucoregulatory activity. *Br. J. Pharmacol.* 163, 399–412.
- (27) Kim, M. Y., Kwon, J. S., Kim, H. J., and Lee, E. K. (2007) In vitro refolding of PEGylated lipase. *J. Biotechnol.* 131, 177–9.
- (28) Seo, J. A., and Kim, N. H. (2012) Fibroblast growth factor 21: a novel metabolic regulator. *Diabetes Metab. J.* 36, 26–8.
- (29) Xiao, J., Burn, A., and Tolbert, T. J. (2008) Increasing solubility of proteins and peptides by site-specific modification with betaine. *Bioconjugate Chem.* 19, 1113–8.
- (30) Manning, M. C., Patel, K., and Borchardt, R. T. (1989) Stability of protein pharmaceuticals. *Pharm. Res.* 6, 903–18.